RESEARCH ARTICLE SUMMARY

FRAMEWORK MATERIALS

Design of higher valency in covalent organic frameworks

Cornelius Gropp, Tianqiong Ma, Nikita Hanikel, Omar M. Yaghi*

INTRODUCTION: Valency is the connectivity of building units in reticular frameworks. Although metal-organic frameworks (MOFs) are known to have valencies of 3 to 24, covalent organic frameworks (COFs) are limited to the lower valencies of 3 and 4, principally owing to the heavy reliance of organic chemistry on sp^2 and sp^3 hybridization. We show that the diversity of COFs can be increased by finding new ways of linking simple organic molecules into building units of higher and even infinite valencies.

RATIONALE: Now, COFs are made by connecting preformed trigonal-planar, square-planar, and tetrahedral organic building units with linkages of low valency. Our strategy is to implement higher valency in COFs by designing molecules capable of forming higher-valency linkages through clustering. This is difficult to achieve by conventional organic methods. We therefore relied on the isoelectronic replacement of carbon-group elements by boron and phosphorus and demonstrated the feasibility of this chemistry by using borophosphonate for the silicate cube motif. We designed simple organic BPA linkers (BPA-**1** to **5**) based on boron and phosphorus, which self-condensed into cubic units and polycubane COFs of valency 8. The versatility of this chemistry was further exploited by cleaving the cubes in the polycubane COFs, leading to structures with rod units of infinite valency.

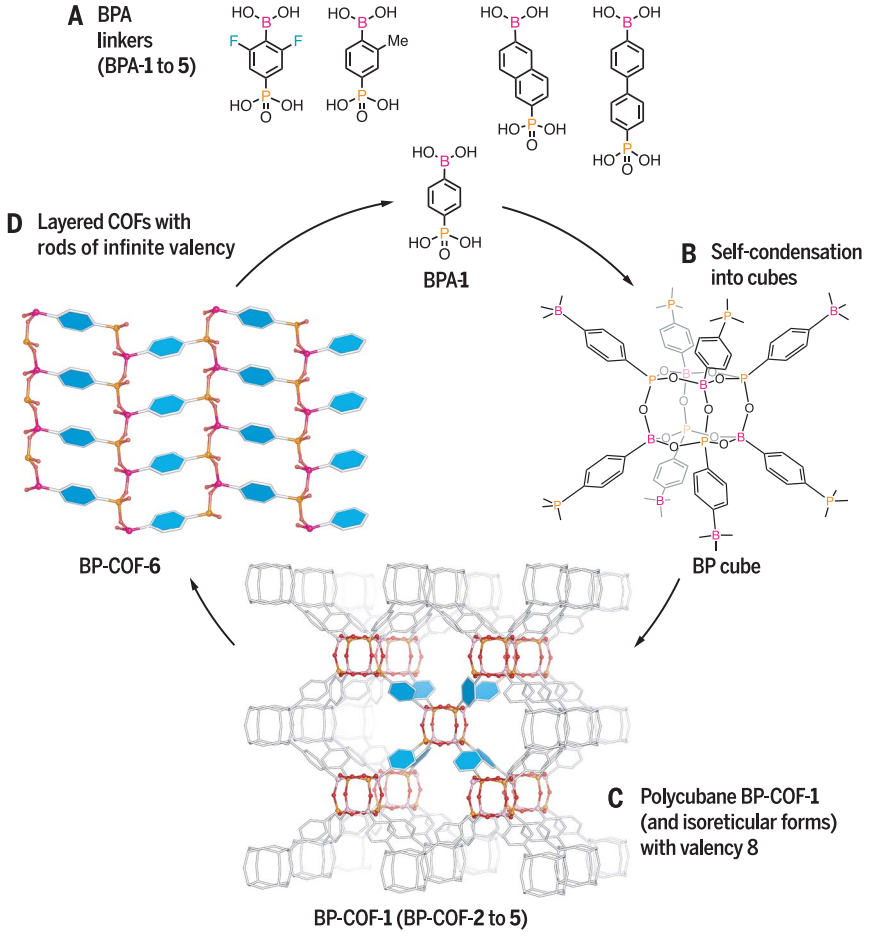

Design of higher valency in COFs from single organic linkers. (**A**) BPA linkers (BPA-**1** to **5**) combine a boronic and a phosphonic acid functionality in a single molecule. (**B** and **C**) Self-condensation of BPA-**1** (B) afforded BP cubes of valency 8 (C) and their reticulated polycubane BP-COF-**1**. Isoreticular forms (BP-COF-**2** to **5**) demonstrated the versatility of this chemistry. (**D**) Upon addition of acid, BP-COF-**1** rearranged into the layered BP-COF-**6**, which exhibits rods of infinite valency.

RESULTS: The BPA-**1** linker combines a boronic acid and a phosphonic acid functionality in a single molecule, which was converged into the boron-phosphorus (BP) cube of a reticulated polycubane BP-COF-**1**. Specifically, eight BPA-**1** linkers self-condensed to form the BP cube with the elimination of eight water molecules per cube. The crystallization of BP-COF-**1** was realized through microscopic reversibility: The polarized B–O–P linkage can dynamically form and break at the B–O bond. This constituted new chemistry whereby simple linkers converged into frameworks composed of higher-valency clusters. The versatility of this strategy was demonstrated by the successful crystallization of isoreticular polycubane structures, BP-COF-**2** to **5** from the BPA-**2** to **5** linkers. This series of functionalized and expanded polycubane structures exhibited permanent porosity. We found that upon addition of acid to BP-COF-**1**, eight B–O bonds per cube were cleaved and rearranged into BP-COF-**6**, which exhibits rods of infinite valency. The structure of BP-COF-**6** was obtained from single-crystal x-ray diffraction, making it one of the few COFs grown as large crystals. It revealed infinite B–O–P rods linked by phenyl units to form layers, which in the crystal were joined by interstitial water molecules acting to stabilize an otherwise unusual rod-within-layer arrangement.

CONCLUSION: The chemistry of BPA linkers and their demonstrated ability to form cubes and higher-valency structures expand the scope of COFs. In essence, BPA linkers were indispensable in making linkages in the form of cubes and rods of higher valency and their corresponding extended BP-COF structures, thereby opening opportunities for the diversification of COFs through clustering of organic molecules based on sp^2 and sp^3-hybridized atoms. The extension of this approach to COFs containing combinations of different shapes promises to uncover what we anticipate is a large, untapped structure space. ■

The list of author affiliations is available in the full article online.
*Corresponding author. Email: yaghi@berkeley.edu
Cite this article as C. Gropp *et al.*, *Science* **370**, eabd6406 (2020). DOI: 10.1126/science.abd6406

READ THE FULL ARTICLE AT
https://doi.org/10.1126/science.abd6406

Downloaded from http://science.sciencemag.org/ on October 22, 2020

RESEARCH ARTICLE

FRAMEWORK MATERIALS

Design of higher valency in covalent organic frameworks

Cornelius Gropp[1,2], Tianqiong Ma[1,2], Nikita Hanikel[1,2], Omar M. Yaghi[1,2]*

The valency (connectivity) of building units in covalent organic frameworks (COFs) has been primarily 3 and 4, corresponding to triangles and squares or tetrahedrons, respectively. We report a strategy for making COFs with valency 8 (cubes) and "infinity" (rods). The linker 1,4-boronophenylphosphonic acid—designed to have boron and phosphorus as an isoelectronic combination of carbon-group elements—was condensed into a porous, polycubane structure (BP-COF-1) formulated as $(-B_4P_4O_{12}-)(-C_6H_4-)_4$. It was characterized by x-ray powder diffraction techniques, which revealed cubes linked with phenyls. The isoreticular forms (BP-COF-2 to 5) were similarly prepared and characterized. Large single crystals of a constitutionally isomeric COF (BP-COF-6), composed of rod units, were also synthesized using the same strategy, thus propelling COF chemistry into a new valency regime.

The development of metal-organic frameworks (MOFs) and covalent organic frameworks (COFs) through reticular chemistry has extended metal-complex and organic chemistries to infinite two- and three-dimensional (2D and 3D) forms (*1*–*6*). The extensive diversity and multiplicity of MOFs are fueled by the variety of valency (connectivity) imparted by their building units. These range from 3 to 24 for discrete units and "infinity" for 1D rods; all are multimetallic entities that, when linked with organics, lead to a vast MOF structure space (*7*). By contrast, the building units in COFs, with few exceptions (*8*), have been entirely based on the valency of 3 and 4, and there are no reports of any infinite dimensionality components linked with organics. This more limited scope of COF chemistry is evidenced by only 18 different structure types (topologies) reported for COFs (*1*, *9*) versus more than 2000 for MOFs (*10*, *11*). Thus, to increase the valency and dimensionality of building units in COFs, there is an interest in finding ways to overcome limitations imposed by the trigonal-planar (sp^2), square-planar (sp^2), and tetrahedral (sp^3) hybridization of organic building units (Fig. 1A).

Isoelectronic replacement as a synthetic strategy to afford higher valency in COFs

Here, we show how an isoelectronic combination of carbon group elements, based on boron and phosphorus that have low valency, can form COFs composed of higher-valency cube and infinite 1D building units (Fig. 1A). We designed a simple organic molecule—borophosphonic acid, BPA-**1**—that combined B and P to make expanded polycubane COFs (Fig. 1B) as well as a COF containing B–O–P rods linked by phenyls. The alternative strategy of using two discrete molecules, each with a different functionality, is commonly practiced in COF chemistry and leads to lower-valency structures. Accordingly, the use of phenyldiboronic acid (BA) and phenyldiphosphonic acid (PA) (Fig. 1B) was unsuccessful, because BA self-condenses into boroxine-linked extended structures that have a valency of 3 (*3*). We report how our strategy of using a single linker bearing the two different functionalities needed for making the desired B–O–P linkages addresses this problem.

Specifically, we designed linkers BPA-**1** to **5** and successfully reticulated them into a 3D COF (BP-COF-**1**), its functionalized forms (BP-COF-**2** and **3**), and its expanded forms (BP-COF-**4** and **5**), all having cubic units and valency of 8 (Fig. 1, B and C). We further elaborated this strategy beyond cubes to show their rearrangement into infinite B–O–P rods linked by organics. The ability to control the reticulation of a single organic linker containing an isoelectronic combination of elements into entities of higher valency and infinite dimensionality adds to the complexity and scope of COFs.

There are two potential strategies to achieve higher valency in COFs. Either a building unit of the desired valency could be made a priori and reticulated, or a designed linker could itself be reticulated to make such a unit in situ. The former is the current conceptual basis of COF chemistry and has led to several structures of valency 6 (*8*). However, this approach requires arduous, multistep syntheses to obtain the building units in a form amenable to COF reactions and, ultimately, crystallization (*12*). In general, this strategy has not been successful in making crystalline structures of diverse constituents, as often observed for linking the silicate cube with organics (Fig. 1D) (*13*).

We instead developed the in situ strategy using the cube motif for making higher-valency COFs. We reasoned that by replacing the Si with its isoelectronic B and P combination, the resulting polarization would allow for the microscopic reversibility and ultimately lead to the desired crystalline COFs (Fig. 1D). The polarized B–O–P linkage can break and form at the O–B bond into the trigonal boronic acid with a vacant p orbital and the corresponding phosphonic acid (Fig. 1D). Both functionalities are readily accessible by synthetic chemistry, but so far, their dynamic covalent bonds have not been explored in reticular chemistry (*14*). Given that BP cube is known as a discrete molecule (*15*, *16*), we targeted the synthesis of the BPA organic linkers and expected that their self-condensation would yield the desired expanded polycubane BP-COFs (Fig. 1B).

Polycubane COFs from linkers containing B and P

BPA-**1** was prepared in two steps from commercially available starting materials and was air stable (section S1 of the supplementary materials). BPA-linkers of varying lengths and functionalities were readily accessed by analogous routes in two to three steps, as demonstrated by the synthesis of BPA-**2** to **5** (Fig. 1C; section S1). The synthesis of BP-COF-**1** is based on the molecular dehydration reaction, in which eight BPA-**1** linkers converge to form the cubic borophosphonate with the elimination of eight water molecules per cube (Fig. 1D). Because the dynamic covalent chemistry for the reversible assembly of BP-type molecules has not been previously explored, we screened various reaction conditions for the condensation of these BPA linkers and used modulators to control the reversibility and thus the periodicity of the reticulated products.

Optimized reaction conditions for this series of COFs were exemplified by the synthesis of BP-COF-**1** and involved dissolving BPA-**1** (20.0 mg, 0.1 mmol) with methylphosphonic acid as modulator (2.5 equiv) in dimethylsulfoxide (0.2 ml) and toluene (0.8 ml). This mixture, containing the dissolved solids but exhibiting solvent phase separation, was sealed in a Pyrex tube and heated at 120°C for 72 hours. BP-COF-**1** was isolated and solvent-exchanged with tetrahydrofuran and methanol, then activated under dynamic vacuum to give the crystalline compound as a white powder in 48% yield (section S1).

The atomic composition of BP-COF-**1** was determined by elemental and inductively coupled plasma analyses and found to correspond to $C_6H_6BO_4P$ within the standard experimental error (section S1). H_2O was replaced by methylphosphonic acid when used as a modulator

[1]Department of Chemistry, University of California–Berkeley, Berkeley, CA 94720, USA. [2]Kavli Energy Nanoscience Institute at UC Berkeley, Berkeley, CA 94720, USA.
*Corresponding author. Email: yaghi@berkeley.edu

Downloaded from http://science.sciencemag.org/ on October 22, 2020

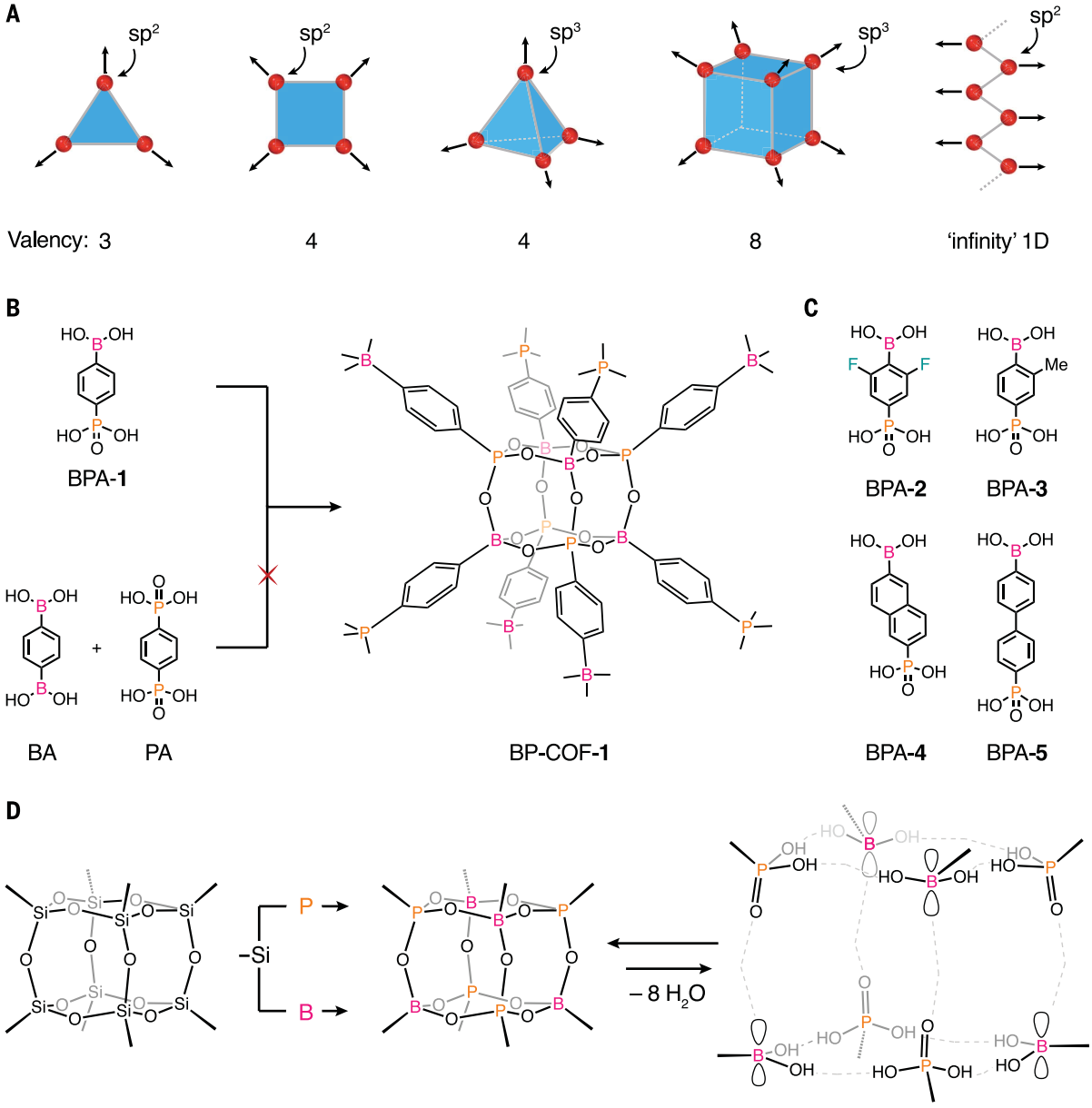

Fig. 1. Higher valency in COFs and synthetic strategy for polycubanes. (**A**) Building units of valency 3 and 4 are currently used in the design and synthesis of 3D COFs; cubes with valency of 8 and infinite 1D rods have not been reported. (**B**) Reticulation of a linker designed to hold two functionalities (BPA-**1**) affords BP-COF-**1** with valency of 8; the alternative strategy involving BA and PA gives instead COFs of lower valency. (**C**) Linkers with different functionalities (BPA-**2** and **3**) and lengths (BPA-**4** and **5**) were prepared and used to make the corresponding COFs. (**D**) Isoelectronic replacement as a conceptual basis for creating reversible in situ formation of the cubic units.

(section S1). The constitution of BP-COF-**1** was corroborated by solution-state nuclear magnetic resonance (NMR) of its acid-digested form, which, as expected, gave back the original BPA-**1** linker (figs. S2 and S3). Thermogravimetric analysis done under both N_2 and air atmosphere indicated that the framework has a thermal stability of up to 500°C with a weight loss of 36%, corresponding to water and the hydrocarbon linker (section S4). The residual compound after combustion was identified as boronphosphate (BPO_4), confirmed by its powder x-ray diffraction (PXRD) pattern, and the observed weight loss matched the proportion of carbon and hydrogen present in the compound and found in the elemental analysis (section S5).

The PXRD analysis confirmed the crystallinity of BP-COF-**1** and revealed no diffraction peaks that could be attributed to residual starting material or reaction additives (Fig. 2A and fig. S49). Scanning electron microscopy (SEM) micrographs of the BP-COF-**1** crystallites indicated a single morphological phase with a homogeneous distribution of crystal sizes of ~300 to 400 nm (Fig. 2B). The formation of the BP cube structure in BP-COF-**1** was supported with characteristic resonances in the Fourier-transformed infrared (FT-IR) and ^{11}B, ^{31}P, and ^{13}C solid-state NMR spectra.

A molecular analog of a borophosphonate cube was prepared and served as a model compound (section S1) (*17*). Diagnostic signals in the FT-IR and NMR spectra of the BP-COF-**1** coincided with those we measured for the model system and were distinct from the BPA-**1** starting material. The absorption bands between 3000 to 3500 cm^{-1} observed for the ν(OH) of the $PO(OH)_2$ and $B(OH)_3$ groups were

Downloaded from http://science.sciencemag.org/ on October 22, 2020

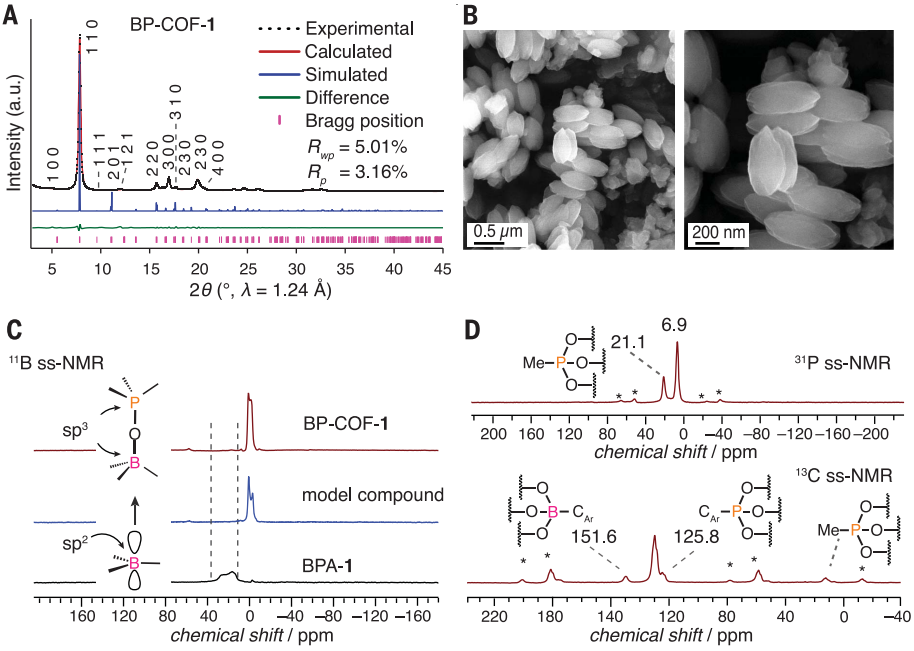

Fig. 2. Structural and molecular characterization of 3D cubic BP-COF-1. (**A**) Structural refinement of BP-COF-**1** from PXRD data analysis displaying the indexed experimental pattern (black), Pawley fitting (red), and the simulated pattern obtained from the modeled structure (blue). a.u., arbitrary units. (**B**) SEM micrographs of BP-COF-**1**. (**C**) Overlay of the ^{11}B solid-state (ss) NMR spectra of BP-COF-**1**, a molecular borophosphonate model compound, and BPA-**1**. (**D**) ^{31}P and ^{13}C NMR spectra of BP-COF-**1**. Me, methyl.

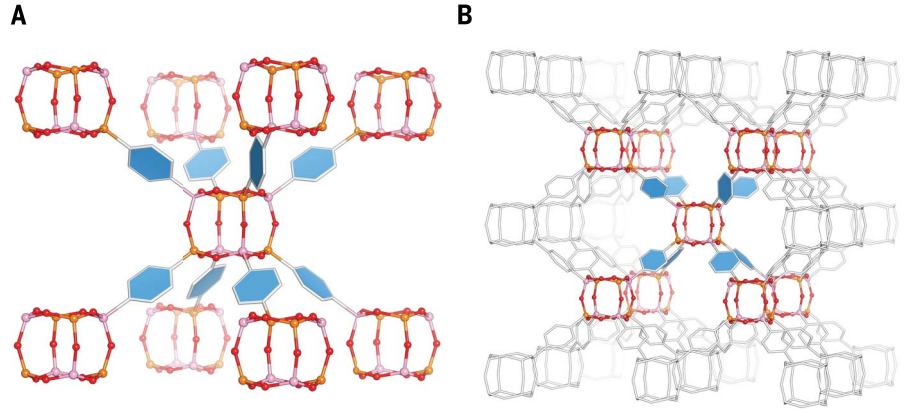

Fig. 3. Crystal structure of BP-COF-1. (**A** and **B**) Crystals of BP-COF-**1** have cubes linked to eight phenyl units bridging to other such cubes (A) to make a 3D extended polycubane COF (B) (bcu; *P*222) with valency of 8. C, gray; B, pink; P, orange; O, red. Hydrogens are omitted for clarity.

absent, indicating a complete reaction and the condensation of these groups to make the COF (fig. S7). Strong absorption bands at 1210, 1140, and 1050 cm^{-1} assigned to the ν(B–O–P) of the cubic BP-COF-**1** are comparable within <5 cm^{-1} to vibrational bands found in the model system and molecular reference structures (figs. S5 and S7) (*18*).

Magic angle spinning (MAS) solid-state NMR spectroscopy of the ^{11}B, ^{31}P, and ^{13}C nuclei was performed to further validate the formation and connectivity of the cubic units (Fig. 2, C and D). The second-order quadrupolar NMR line shape of the ^{11}B nucleus is a sensitive probe to substantiate the conversion of the trigonal-planar boron site of the starting material (in BPA-**1**) into the tetrahedral boron site of the product (BP-COF-**1**) (*19*). Comparison of the experimental second-order quadrupolar line shapes of the ^{11}B NMR resonances of the starting material BPA-**1** and the model system with BP-COF-**1** supported the presence of tetrahedral boron sites in both products (Fig. 2C and section S6). The single resonance in the ^{11}B NMR spectrum of BP-COF-**1** indicated negligible defect sites within the crystallites.

The ^{31}P spectrum of BP-COF-**1** displayed two discrete peaks, a major resonance at 6.9 parts per million (ppm) and a minor one at 21.1 ppm, indicating two distinct P sites. The latter resonance was assigned to residual modulator molecules, methylphosphonates, located at the terminal site of the crystallites. The ^{13}C cross-polarization MAS NMR spectrum displayed discrete resonances in the aromatic region between 151.6 and 125.8 ppm (Fig. 2D). We assigned the resonance at 151.6 ppm to the downfield-shifted carbon bonded to the tetrahedral boron and the peak at 125.8 ppm to the carbon connected to the phosphorus. The relative shifts match well with the ones observed for the molecular model compound, further supporting the formation of the cube units in the COF (section S6) (*17*, *18*).

The crystal structure of BP-COF-**1** was obtained by PXRD analysis of its microcrystalline powder. For BP-COF-**1**, linking of the borophoshonate cubes with eight benzene bridges affords a cubic extended structure based on the body-centered cubic (bcu) topology (Fig. 3 and fig. S55). The distance between the centers of adjacent cubes was 11.128 Å, which includes a distance of 6.228 Å between B and P on adjacent cubes, being bridged by the phenyl units (section S8). A structural model based on a bcu arrangement was built in the *P*222 space group with the optimized unit cell parameters of a = 12.800 Å, b = 12.915 Å, and c = 12.798 Å. The corresponding simulated PXRD pattern was in good agreement with the experimentally obtained data (Fig. 2A). Pawley refinement of the experimental PXRD pattern yielded the refined unit cell parameters of a = 12.39(5) Å, b = 12.52(3) Å, and c = 12.93(5) Å, with the unweighted reliability factor (R_p) = 5.01% and the weighted reliability factor (wR_p) = 3.16%, and the final structure was obtained by geometry optimization. The corresponding crystal structure has $B_4P_4O_{12}$ cubes each covalently linked to eight phenyl units, acting as bridges to other such linked cubes to give an overall reticular formula of $(-B_4P_4O_{12}-)(-C_6H_4-)_4$ for the extended 3D polycubane porous structure of BP-COF-**1** (Fig. 3).

The N_2 adsorption analysis of BP-COF-**1** demonstrated permanent porosity and a Type I behavior (section S10). The Brunauer-Emmett-Teller (BET) area was calculated to be 519 m^2 g^{-1}, corresponding to ~82% of the theoretically accessible surface area based on the crystal structure (section S11). This result was validated by argon adsorption analysis at 87 K (fig. S63). The pore size distribution, estimated from the N_2 isotherm by a density functional theory (DFT) calculation, indicated a pore diameter of 6.0 Å (section S11), which is in good agreement with the theoretical van der Waals distance of 5.8 Å obtained from the crystal structure. Importantly, H_2 isotherms

Downloaded from http://science.sciencemag.org/ on October 22, 2020

at 77 and 87 K for BP-COF-**1** also demonstrated the accessibility of the cubic unit for gas sorbates. The experimental gravimetric uptake of H_2 at 1 atm and 77 K measured 11.6 mg g^{-1} (volumetric uptake 130 cm^3 g^{-1} at 1 atm; fig. S65). The heat of adsorption (Q_{st}) was ~8.8 kJ mol^{-1}, indicating stronger sorbate-framework interactions than comparable boroxine-linked 2D and 3D COFs (*20*). We attributed the stronger interactions to the polarized nature of the pore environment replete with accessible B–O–P edges of the cubes that make up the structure of BP-COF-**1**, an aspect that also points to the effectiveness of placing lower-valency atoms into constructs of higher valency within COFs.

Isoreticular forms of polycubane COFs

We extended the approach of having a single linker converge into a high-valency building unit to the synthesis and structure of functionalized and expanded versions of BP-COF-**1** by introducing functional groups into BPA-**1** to make BPA-**2** and **3**, as well as expanding the linkers to BPA-**4** and **5** (Fig. 1C). The corresponding COFs (BP-COF-**2** to **5**) were synthesized and characterized as demonstrated for BP-COF-**1**; they followed the expected pattern of isoreticulation (*21*) and exhibited similar spectroscopic and x-ray evidence (sections S3 and S6 to S8). In particular, the expanded isoreticular series (BP-COF-**1**, **4**, and **5**) showed a shift to higher *d*-spacing in the PXRD, corresponding to the change in length of the organic units and its impact on the unit cell dimensions (Fig. 4A). A gradual shift of the lowest angle diffraction peak in each of the patterns toward smaller 2θ values was observed (Fig. 4B), in agreement with the increase in linker length measured from B to P of 6.2, 8.4, and 10.5 Å for the phenyl, naphthyl, and biphenyl, which are BPA-**1**, **4**, and **5**, respectively (Fig. 4B). Based on our success with these cubic COFs, we anticipate other linkers, such as the tetrahedral form of BPA and combinations based on other shapes, to give a wide range of higher-valency structures (*22*).

Single crystals of a constitutionally isomeric COF with rod units of infinite valency

In an effort to further explore the condensation reaction of BPA-**1** into structures with building units beyond cubes, we investigated the use of reaction additives, such as acids and bases. Under similar reaction conditions used for the synthesis of BP-COF-**1**, but in the presence of 20 μl of aqueous $HCl_{conc.}$, we obtained a new crystalline phase, BP-COF-**6**, as confirmed by PXRD (fig. S50). Single crystals of 50 μm with well-defined, uniform block-shaped morphology were obtained and examined by single-crystal x-ray diffraction techniques (Fig. 5). BP-COF-**6** crystallized in the *Pc* space group with unit cell parameters of a = 5.4728(16) Å, b = 4.3774(12) Å, c = 14.285(4) Å, and β = 95.402(7)° and a unit cell volume of 340.71(16) $Å^3$ (Fig. 5 and table S2). Structure analysis showed that the cubic borophosphonates were replaced by infinite 1D B–O–P rods of alternating tetrahedral boron and phosphorus building units. The B–O–P bond lengths within the 1D rod were 1.47(3) Å (B–O) and 1.54(1) Å (P–O). These 1D rods were connected by phenyls that had interlayer spacings of 5.47 Å (measured from phenyl to phenyl). This distance exceeded π-π–stacking distances because of the water molecule connecting the layers through hydrogen bonding (H bonding). The layers were stacked along the *a* axis and followed a honeycomb pattern (hcb). The B–O–P rods were oriented along the *b* axis with the uncondensed P=O groups unidirectionally aligned along the −*a* axis. The O···O distances of 2.58 and 2.60 Å between the P=O and the oxygen at the boron indicated strong hydrogen bonds, most likely stemming from interstitial water molecules strongly bound to the boron and enforcing the tetrahedral geometry (Fig. 5).

The P–O distances of 1.46(2) Å support a P=O double-bond character, and the B–O distance of 1.60(4) Å supports a strong dative bonding of the water molecule donating electron density into the empty p orbital of the boron. This H-bonding sequence connected the extended 2D layers of BP-COF-**6**, whose framework was formulated as (–BPO_4–)(–C_6H_4–). This structure motif of B–O–P rods linked by organics led to infinite valency COFs. In the context of single crystals of COFs, there have been several studies of solving crystal structures using electron diffraction (*23*, *24*); however, the single-crystal x-ray structure of BP-COF-**6** is one of only a few reported in COF chemistry (*25*, *26*).

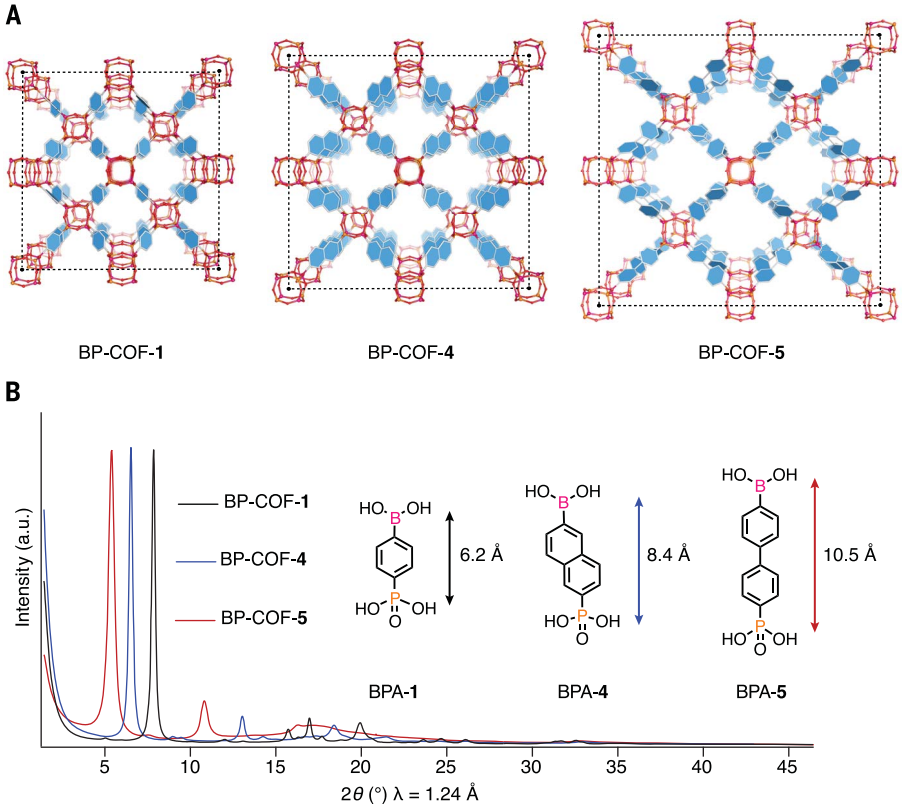

Fig. 4. Isoreticular expansion of BP-COFs. (**A**) Isoreticular series (BP-COF-**1**, **4**, and **5**) demonstrates the generalizability of the in situ approach. Expansion of the unit cell is illustrated by black dotted lines. (**B**) With increasing length of the BPA linkers, a shift of the highest intensity PXRD peak (110) toward lower 2θ (°) was observed. C, gray; B, pink; P, orange; O, red. Hydrogens are omitted for clarity.

Discussion: Rearrangement of polycubane COFs into rod COFs

Elemental analysis, solution NMR of the acid-digested sample, and thermogravimetric analysis of BP-COF-**6** confirmed that this compound had identical elemental composition to BP-COF-**1** and that they were constitutional isomers (sections S1 and S2). We found that cubic BP-COF-**1** could be fully interconverted into the rod BP-COF-**6** in the presence of 20 μl of aqueous $HCl_{conc.}$ (Fig. 6), as evidenced by PXRD (section S1 and fig. S54). We suggest that the strongly bonded, interstitial water molecule at the center of the H bonding between the layers of BP-COF-**6** results from hydrolysis (bond breaking) after addition of acid, followed by condensation producing water as a by-product,

Downloaded from http://science.sciencemag.org/ on October 22, 2020

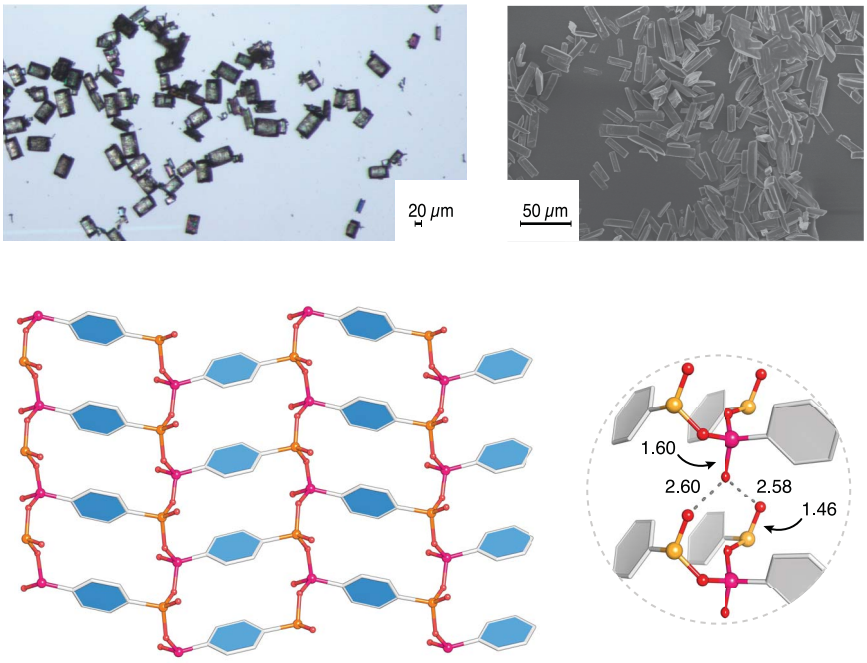

Fig. 5. Single-crystal x-ray diffraction structure of BP-COF-6, which has units of infinite valency. Optical microscope (top left) and SEM (top right) images of BP-COF-**6**. A layer in the single-crystal x-ray structure of BP-COF-**6** (bottom left). Local H-bonding interactions between the layers are indicated in O···O distances between O on P and B and are given in Å (bottom right). C, gray; B, pink; P, orange; O, red. Hydrogens on the phenyl units and the tightly bound water ligands bound to B atoms are omitted for clarity.

facilitating this clean transformation. Thus, the interconversion potentially follows a breaking of the B–O bonds in the horizontal B–O–P linkages of the cube, keeping the vertical ones untouched and thereby producing B–O–P–phenyl "chains" following the 1, 2, 3, … sequence (Fig. 6A). Thus, BP-COF-**1** can be viewed as being composed of a collection of such chains, which, owing to the bond breaking, are now liberated to slide toward each other in pairs (1, 2, 3, … and 1′, 2′, 3′, …; Fig. 6A) and form the B–O–P rod arrangement (1, 1′, 2, 2′, 3, 3′, …; Fig. 6B) poised for condensation, to ultimately give the rod BP-COF-**6** (Fig. 6C). That the P=O bonds remaining after B–O bond breaking all pointed in the same direction supported our model of how this rearrangement took place. The tightly bound water molecules at the boron may very well be playing a stabilizing role in trapping the rod units in BP-COF-**6**, especially because such rods were previously unknown. This type of rearrangement is distinct in the chemistry of B and P and is a result of the polarized B–O–P linkage, which, on the basis of this report, promises rich chemistry.

Materials and methods

Full experimental details and characterization of BPA-**1** to **5** and BP-COF-**1** to **6** are provided in sections S1 to 13 of the supplementary materials.

Synthesis of BP-COF-1

A Pyrex tube measuring 10 mm by 8 mm [outside diameter (od) by inside diameter (id)] was loaded with BPA-**1** (20 mg, 0.10 mmol), methylphosphonic acid (24 mg, 0.25 mmol), 0.2 ml of dimethyl sulfoxide (DMSO), and 0.8 ml of toluene. The tube was flash frozen at 77 K under liquid N_2, evacuated to an internal pressure of 100 mtorr, and flame-sealed to a length of 15 cm, approximately. The tube was placed in an oven at 120°C for 72 hours, yielding a white solid. The solvent was removed, and the residual solid was immersed once in 5 ml of tetrahydrofuran and three times in 5 ml of methanol over 24 hours. The solid was activated under dynamic vacuum, first at 25°C for 5 hours and then at 150°C for 6 hours. BP-COF-**1** (6.9 mg, 48%) was obtained as a white powder.

Synthesis of BP-COF-6

A Pyrex tube measuring 10 mm by 8 mm (od by id) was loaded with BPA-**1** (10 mg, 0.05 mmol), 20 μl of $HCl_{conc.}$, 0.2 ml of DMSO, and 0.8 ml of toluene. The tube was sealed and placed in an oven at 120°C for 5 days, yielding a white solid. The solvent was removed, and the residual solid was immersed once in 5 ml of tetrahydrofuran and three times in 5 ml of methanol over 48 hours. The solid was then activated under dynamic vacuum, first at 25°C for 5 hours and then at 150°C for 6 hours. BP-COF-**6** (5.0 mg, 60%) was obtained as a white powder.

Conversion of BP-COF-1 into BP-COF-6

A Pyrex tube measuring 10 mm by 8 mm (od by id) was loaded with BP-COF-**1** (10 mg, 0.05 mmol), 20 μl of $HCl_{conc.}$, 0.2 ml of DMSO, and 0.8 ml of toluene. The tube was sealed and placed in an oven at 120°C for 72 hours, yielding a white solid. The solvent was removed, and the residual solid was immersed once in 5 ml of tetrahydrofuran and three times in 5 ml of methanol over 24 hours. The solid was then activated under dynamic vacuum, first at 25°C for 5 hours and then at 150°C for 6 hours. BP-COF-**6** was obtained as a pure phase, as confirmed by PXRD.

PXRD

PXRD patterns of BP-COF-**1** to **6** were acquired on an in-house Bruker D8 Advance equipped with a Ni filter CuKα (λ = 1.5406 Å) or on the beamline 7.3.3 at the Advanced Light Source with a Pilatus 2M detector (λ = 1.2389 Å). For in-house measurements, the samples were mounted on zero-background sample holders and leveled with a glass plate. Some samples were grinded in an agata mortar before analysis. Data were collected between 3° and 50° or 60° with a step width of 0.01 and a total data collection time of 4 to 5 hours. For beamline measurements, powder samples were packed in quartz capillaries and put into a helium atmosphere for measurement in transmission geometry. Silver behenate was used for calibration. The Nika package for IGOR Pro (Wavemetrics) was used to reduce the acquired 2D raw data to a 1D profile (*27*). Refinements were conducted with the Material Studio (version 4.0, Accelrys, San Diego, CA) (*28*).

Single-crystal x-ray diffraction

A colorless block-shaped crystal of BP-COF-**6** was measured at the beamline 12.2.1 at the Advanced Light Source using a radiation wavelength of λ = 0.7288 Å. The crystal was mounted on a MiTeGen Kapton loop and submerged in a 100-K nitrogen cryostream for the measurement. The data reduction was carried out with APEXII (*29*) software packages. The structure solution and refinement were carried out using the SHELX algorithms (*30*) in Olex2 (*31*). Crystal data and details of the structure refinement are given in table S1 and in the provided cif file (data S1). Mercury was used for structural visualization (*32*).

Low-pressure gas sorption

Low-pressure argon, N_2, and H_2 adsorption isotherm measurements of BP-COF-**1** to **6** were carried out on a Micromeritics 3-Flex or an

Downloaded from http://science.sciencemag.org/ on October 22, 2020

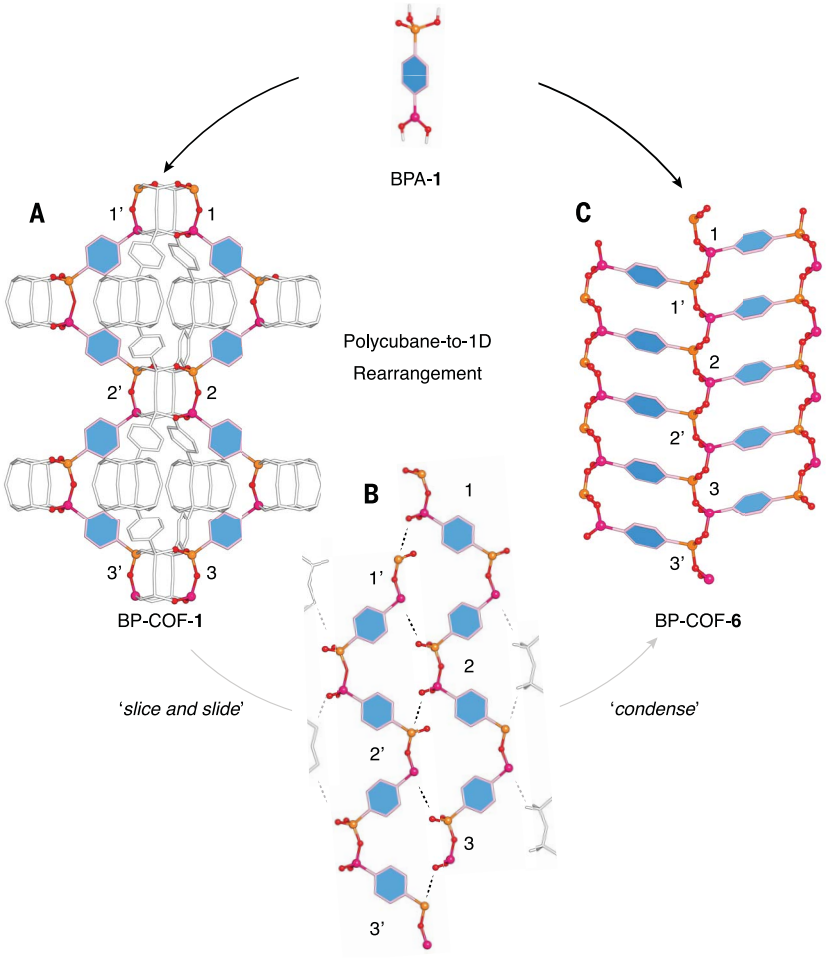

Fig. 6. Polycubane-to-1D rearrangement of BP-COF-1 to BP-COF-6. (**A** to **C**) Suggested mechanism for the interconversion of the cubic BP-COF-**1** into the layered BP-COF-**6** through a "slice-and-slide"–type rearrangement and condensation. C, gray; B, pink; P, orange; O, red. Hydrogens are omitted for clarity.

ASAP 2420 surface area analyzer. A liquid N_2 bath was used for measurements at 77 K. A liquid argon bath was used for measurements at 87 K. Ultrahigh-purity-grade N_2, argon, H_2, and He (99.999% purity) were used throughout adsorption experiments. Solvent-accessible surface areas were calculated with Material Studio (version 4.0, Accelrys, San Diego, CA) (*28*) using a N_2- or argon-sized probe molecule (of diameters 3.68 and 3.96 Å, respectively) and a grid interval of 0.25 Å (*33*). The pore size was calculated with MicroActive (version 5.01) (*34*) from the N_2 or argon isotherms by applying a DFT type, slit geometry, 2D-NLDFT, N2-Carbon Finite Pores, As=4 Model for nitrogen isotherms, and a DFT type, slit geometry, AR-DFT Model for argon isotherms. The theoretical van der Waals distance was deduced from the model by measuring the heavy atom van der Waals distances. Experimental BET areas were calculated from the respective isotherms with data from the low-pressure range ($P/P_0 \leq 0.1$; see section S10), with pressure points as low as 10^{-7} P/P_0. The correlation coefficients and positive C values are given in section S10 for each BET calculation.

REFERENCES AND NOTES

1. O. M. Yaghi, M. J. Kalmutzki, C. S. Diercks, *Introduction to Reticular Chemistry: Metal-Organic Frameworks and Covalent Organic Frameworks* (Wiley, 2019).
2. O. M. Yaghi *et al*., Reticular synthesis and the design of new materials. *Nature* **423**, 705–714 (2003). doi: 10.1038/nature01650; pmid: 12802325
3. A. P. Côté *et al*., Porous, crystalline, covalent organic frameworks. *Science* **310**, 1166–1170 (2005). doi: 10.1126/science.1120411; pmid: 16293756
4. H. M. El-Kaderi *et al*., Designed synthesis of 3D covalent organic frameworks. *Science* **316**, 268–272 (2007). doi: 10.1126/science.1139915; pmid: 17431178
5. K. Geng *et al*., Covalent organic frameworks: Design, synthesis, and functions. *Chem. Rev.* **120**, 8814–8933 (2020). doi: 10.1021/acs.chemrev.9b00550; pmid: 31967791
6. C. S. Diercks, O. M. Yaghi, The atom, the molecule, and the covalent organic framework. *Science* **355**, eaal1585 (2017). doi: 10.1126/science.aal1585; pmid: 28254887
7. M. J. Kalmutzki, N. Hanikel, O. M. Yaghi, Secondary building units as the turning point in the development of the reticular chemistry of MOFs. *Sci. Adv.* **4**, eaat9180 (2018). doi: 10.1126/sciadv.aat9180; pmid: 30310868
8. S. Dalapati *et al*., Rational design of crystalline supermicroporous covalent organic frameworks with triangular topologies. *Nat. Commun.* **6**, 7786 (2015). doi: 10.1038/ncomms8786; pmid: 26178865
9. X. Guan, F. Chen, Q. Fang, S. Qiu, Design and applications of three dimensional covalent organic frameworks. *Chem. Soc. Rev.* **49**, 1357–1384 (2020). doi: 10.1039/C9CS00911F; pmid: 32067000
10. E. V. Alexandrov, V. A. Blatov, A. V. Kochetkov, D. M. Proserpio, Underlying nets in three-periodic coordination polymers: Topology, taxonomy and prediction from a computer-aided analysis of the Cambridge Structural Database. *CrystEngComm* **13**, 3947–3958 (2011). doi: 10.1039/c0ce00636j
11. V. A. Blatov, A. P. Shevchenko, D. M. Proserpio, Applied topological analysis of crystal structures with the program package ToposPro. *Cryst. Growth Des.* **14**, 3576–3586 (2014). doi: 10.1021/cg500498k
12. J. Jiang, Y. Zhao, O. M. Yaghi, Covalent chemistry beyond molecules. *J. Am. Chem. Soc.* **138**, 3255–3265 (2016). doi: 10.1021/jacs.5b10666; pmid: 26863450
13. W. Chaikittisilp, A. Sugawara, A. Shimojima, T. Okubo, Hybrid porous materials with high surface area derived from bromophenylethenyl-functionalized cubic siloxane-based building units. *Chem. Eur. J.* **16**, 6006–6014 (2010). doi: 10.1002/chem.201000249; pmid: 20391584
14. S. J. Rowan, S. J. Cantrill, G. R. L. Cousins, J. K. M. Sanders, J. F. Stoddart, Dynamic covalent chemistry. *Angew. Chem. Int. Ed.* **41**, 898–952 (2002). doi: 10.1002/1521-3773(20020315)41:6<898::AID-ANIE898>3.0.CO;2-E; pmid: 12491278
15. M. G. Walawalkar, R. Murugavel, H. W. Roesky, H.-G. Schmidt, The first molecular borophosphonate cage: Synthesis, spectroscopy, and single-crystal x-ray structure. *Organometallics* **16**, 516–518 (1997). doi: 10.1021/om960995n
16. K. Diemert, U. Englert, W. Kuchen, F. Sandt, A cage molecule with a cubanoid P_4B_4 framework: $tBu_4P_4Ph_4B_4O_{12}$—A structural analogue of the isovalence electronic organosilasesquioxanes $R_8Si_8O_{12}$. *Angew. Chem. Int. Ed.* **36**, 241–243 (1997). doi: 10.1002/anie.199702411
17. J. Tönnemann *et al*., Borophosphonate cages: Easily accessible and constitutionally dynamic heterocubane scaffolds. *Chem. Eur. J.* **18**, 9939–9945 (2012). doi: 10.1002/chem.201201287; pmid: 22764094
18. M. G. Walawalkar, R. Murugavel, H. W. Roesky, H.-G. Schmidt, Syntheses, spectroscopy, structures, and reactivity of neutral cubic group 13 molecular phosphonates. *Inorg. Chem.* **36**, 4202–4207 (1997). doi: 10.1021/ic970346j
19. H. Höpfl, The tetrahedral character of the boron atom newly defined—A useful tool to evaluate the N→B bond. *J. Organomet. Chem.* **581**, 129–149 (1999). doi: 10.1016/S0022-328X(99)00053-4
20. H. Furukawa, O. M. Yaghi, Storage of hydrogen, methane, and carbon dioxide in highly porous covalent organic frameworks for clean energy applications. *J. Am. Chem. Soc.* **131**, 8875–8883 (2009). doi: 10.1021/ja9015765; pmid: 19496589
21. M. Eddaoudi *et al*., Systematic design of pore size and functionality in isoreticular MOFs and their application in methane storage. *Science* **295**, 469–472 (2002). doi: 10.1126/science.1067208; pmid: 11799235
22. RCSR, The reticular chemistry structure resource; http://rcsr.net [accessed 26 June 2020].
23. Y.-B. Zhang *et al*., Single-crystal structure of a covalent organic framework. *J. Am. Chem. Soc.* **135**, 16336–16339 (2013). doi: 10.1021/ja409033p; pmid: 24143961
24. A. M. Evans *et al*., Seeded growth of single-crystal two-dimensional covalent organic frameworks. *Science* **361**, 52–57 (2018). doi: 10.1126/science.aar7883; pmid: 29930093
25. T. Ma *et al*., Single-crystal x-ray diffraction structures of covalent organic frameworks. *Science* **361**, 48–52 (2018). doi: 10.1126/science.aat7679; pmid: 29976818
26. L. Liang *et al*., Non-interpenetrated single-crystal covalent organic frameworks. *Angew. Chem. Int. Ed.* **59**, 17991–17995 (2020). doi: 10.1002/anie.202007230; pmid: 32648325
27. J. Ilavsky, *Nika*: Software for two-dimensional data reduction. *J. Appl. Cryst.* **45**, 324–328 (2012). doi: 10.1107/S0021889812004037
28. Dassault Systèmes, BIOVIA Materials Studio 2017 (Waltham, MA, 2016).
29. Bruker AXS Inc., APEX2 (Madison, WI, 2010).
30. G. M. Sheldrick, A short history of SHELX. *Acta Crystallogr. A* **64**, 112–122 (2008). doi: 10.1107/S0108767307043930; pmid: 18156677
31. O. V. Dolomanov, L. J. Bourhis, R. J. Gildea, J. A. K. Howard, H. Puschmann, OLEX2: A complete structure solution, refinement and analysis program. *J. Appl. Cryst.* **42**, 339–341 (2009). doi: 10.1107/S0021889808042726
32. C. F. Macrae *et al*., Mercury: Visualization and analysis of crystal structures. *J. Appl. Cryst.* **39**, 453–457 (2006). doi: 10.1107/S002188980600731X

Downloaded from http://science.sciencemag.org/ on October 22, 2020

33. T. Düren, F. Millange, G. Férey, K. S. Walton, R. Q. Snurr, Calculating geometric surface areas as a characterization tool for metal–organic frameworks. *J. Phys. Chem. C* **111**, 15350–15356 (2007). doi: 10.1021/jp074723h
34. Micromeritics Instrument Corporation, MicroActive, version 5.01 (Norcross, GA, 2018).

ACKNOWLEDGMENTS

We thank T. Zeng and Y.-B. Zhang for support from the SPST Analytical Instrumentation Center (no. SPST-AIC10112914) at ShanghaiTech University for solid-state NMR measurement during the COVID-19 lockdown. C.G. thanks P. Waller and T. Osborn Popp for discussions in the early stages of the project and H. Lyu, X. Pei, and H. L. Nguyen for advice during the entire project. T.M. and N.H. thank X. Pei for helpful discussions on structure refinements. C.G., T.M., N.H., and O.M.Y. thank C. Zhu for acquiring PXRD data on beamline 7.3.3 of the Advanced Light Source. **Funding:** We acknowledge the College of Chemistry Nuclear Magnetic Resonance Facility for resources and staff assistance, where instruments are partially supported by NIH S10OD024998. This research used beamline 7.3.3 and resources of beamline 12.2.1 at the Advanced Light Source, which are U.S. Department of Energy, Office of Science User Facilities, under contract no. DE-AC02-05CH11231. C.G., a Leopoldina postdoctoral fellow of the German National Academy of Science (LPDS 2019-02), acknowledges the receipt of a fellowship of the Swiss National Science Foundation (P2EZP2-184380). N.H. thanks the Studienstiftung des deutschen Volkes and acknowledges receipt of the KAVLI ENSI Philomathia Graduate Student Fellowship. O.M.Y. acknowledges support and collaboration as part of the UC Berkeley–KACST Joint Center of Excellence for Nanomaterials for Clean Energy Applications, King Abdulaziz City for Science and Technology, Riyadh 11442, Saudi Arabia. C.G. and O.M.Y. intend to file a patent application on the reported work. **Author contributions:** C.G. and O.M.Y. conceived the idea and led the project. C.G. synthesized BPA-**1** to **5** and BP-COF-**1** to **5** and conducted the spectroscopic (IR and NMR), thermal gravimetric analysis, and elemental analysis characterizations. T.M. conducted the synthesis of BP-COF-**6** and carried out all PXRD refinements and structural modeling. T.M. and N.H. solved the single-crystal x-ray crystal structure of BP-COF-**6**. N.H. conducted sorption experiments. C.G., T.M., N.H., and O.M.Y. interpreted the results, and C.G., T.M., and O.M.Y. wrote the manuscript. **Competing interests:** None declared. **Data and materials availability:** Synthetic procedures, spectroscopic (IR and NMR), thermal gravimetric analysis, and x-ray diffraction data reported in this manuscript are present in the main text or in the supplementary materials. Unit cell parameters and atomic positions of BP-COF-**1** to **5** are provided as xyz files (data S2). The crystallographic data are tabulated in the supplementary materials and archived at the Cambridge Crystallographic Data Centre under reference number CCDC 2013495.

SUPPLEMENTARY MATERIALS

2 July 2020; accepted 3 September 2020
10.1126/science.abd6406

Downloaded from http://science.sciencemag.org/ on October 22, 2020

Science

Design of higher valency in covalent organic frameworks

Cornelius Gropp, Tianqiong Ma, Nikita Hanikel and Omar M. Yaghi

Science **370** (6515), eabd6406.
DOI: 10.1126/science.abd6406

Higher-valency ligands for COFs

Metal-organic frameworks (MOFs) have exhibited more extensive connectivity (valency) and topological diversity than covalent organic frameworks (COFs), mainly because MOF linkers can connect from 3 to 24 discrete units or even infinity for one-dimensional rods. For COFs, linkers generally have a valency of 3 or 4 that reflect the valency of organic carbon. Gropp *et al.* created cubane-like linkers from 1,4-boronophenylphosphonic acid that could condense to make COFs with a valency of 8 or, by adding acid, could form large, single crystals with an infinite-rod topology.

Science, this issue p. eabd6406

ARTICLE TOOLS http://science.sciencemag.org/content/370/6515/eabd6406

SUPPLEMENTARY MATERIALS http://science.sciencemag.org/content/suppl/2020/10/21/370.6515.eabd6406.DC1

REFERENCES This article cites 31 articles, 7 of which you can access for free
http://science.sciencemag.org/content/370/6515/eabd6406#BIBL

PERMISSIONS http://www.sciencemag.org/help/reprints-and-permissions

Use of this article is subject to the Terms of Service

Science (print ISSN 0036-8075; online ISSN 1095-9203) is published by the American Association for the Advancement of Science, 1200 New York Avenue NW, Washington, DC 20005. The title *Science* is a registered trademark of AAAS.

Copyright © 2020 The Authors, some rights reserved; exclusive licensee American Association for the Advancement of Science. No claim to original U.S. Government Works

Downloaded from http://science.sciencemag.org/ on October 22, 2020